2013

Joint routing and charging to elongate sensor network lifetime

Zi Li
Iowa State University

Joint routing and charging to elongate sensor network lifetime

by

Zi Li

A thesis submitted to the graduate faculty

in partial fulfillment of the requirements for the degree of

MASTER OF SCIENCE

Major: Computer Science

Program of Study Committee:

Wensheng Zhang, Co-major Professor

Daji Qiao, Co-major Professor

Ting Zhang

Iowa State University

Ames, Iowa

2012

TABLE OF CONTENTS

LIST OF TABLES

LIST OF FIGURES

CHAPTER 1. Introduction

1.1 Wireless Charging Technology

Wireless sensor networks consist of spatially distributed sensor nodes to monitor surrounding environmental conditions, such as temperature, sound, motion of pollutants etc and cooperatively pass their data through the network to a base station (BS). They have been widely employed in a broad range of applications Mainwaring et al. (2002); Xu et al. (2004); Lee et al. (2009); Chipara et al. (2010); Ma et al. (2008) and many of them require long term operation. However, sensor nodes are usually powered by small batteries and the scarce energy supply has constrained its lifetime. This has been a long-lasting, fundamental problem faced by sensor networks. To resolve this problem, various approaches like energy conservation Chang and Tassiulas (2000); Li et al. (2001), ambient energy harvesting Kansal et al. (2004); Fan et al. (2008); Park and Chou (2006); Jose et al. (2001), incremental deployment Tong et al. (2009a), and battery replacement Tong et al. (2009b) have been proposed. However, energy conservation schemes can only slow down energy consumption but not compensate energy depletion. Harvesting environmental energy, such as solar Kansal et al. (2004); Fan et al. (2008), wind Park and Chou (2006) and vibration Jose et al. (2001), is subject to their availability which is often uncontrollable by people. The incremental deployment approach may not be environmentally friendly because deserted sensor nodes can pollute the environment. The battery or node replacement approach is applicable only for scenarios that sensor nodes are accessible by people or sophisticated robots that can locate and physically touch the sensor nodes. Complementary to aforementioned approaches, the emerging wireless charging technology, together with more and more mature and inexpensive mobile robots, creates a perpetual power source to provide power-over-distance and controllable wireless power without requiring accurate localization or

strict alignment between the charger and sensor nodes.

1.2 Joint Routing and Charging Scheduling Problem

Introducing wireless charging technology into sensor networks adds a new dimension to network protocol design. To maximize the lifetime of the wireless chargeable sensor network (WCSN) which is the integration of a sensor network and mobile chargers (MCs), sensor node behaviors and charging activities scheduling should be considered jointly. As sensor networks need to pass the collected data to the base station in a hop-by-hop manner, routing strategy has significant impacts on nodal energy distribution and hence network lifetime. Therefore, in this thesis, we study the joint routing and charging scheduling problem.

Figure 1.1 shows an example of the studied problem. In this figure, sensor nodes

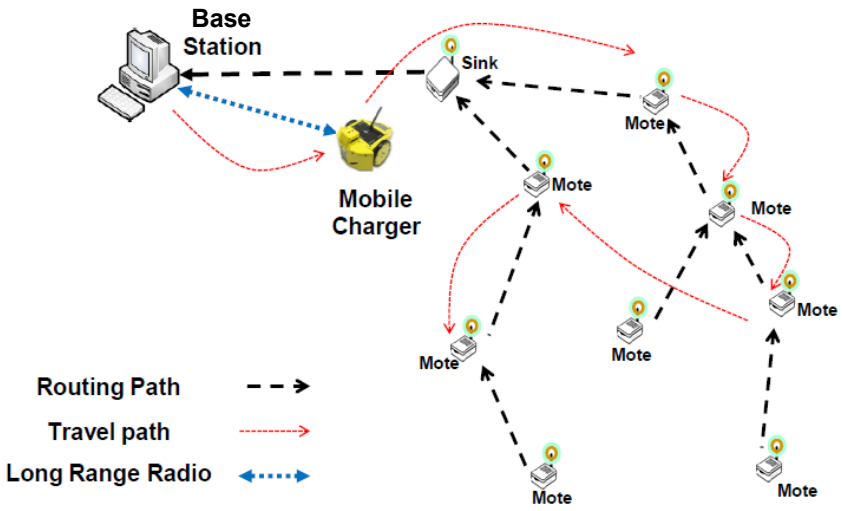

Figure 1.1 An example of joint routing and charging scheduling problem.

collaboratively route the sensory data to the base station while the mobile charger move in the network and transfer energy to nodes nearby. By assuming every sensor node could be charged, it is of fundamental importance to design schemes that can (i) make routing decision for individual nodes and (ii) schedule the charging sequence for the MC, so as to maximize the network lifetime. Such schemes should adapt to the dynamism in charging capabilities, network workload, link conditions, etc, and should have low operational overhead.

To solve this problem, we propose a practical and efficient *J*oint *Ro*uting and *C*harging scheme, named J-RoC, to prolong the network lifetime. To evaluate its performance, we conduct experiments in a testbed consists of TelosB sensor nodes and Powercast Powercast () wireless charger plus Garcia Garcia () robots. Evaluation results demonstrate that J-RoC significantly elongates the network lifetime compared to existing wireless charging based schemes.

1.3 Thesis Outline

The rest of the thesis is organized as follows. Chapter 2 reviews the related research that has been done. Chapter 3 describes the J-RoC design details. In Chapter 4, we will present testbed experiments and simulation results. Chapter 5 concludes this thesis.

CHAPTER 2. Survey of Literature

Employing two strongly coupled magnetic resonant objects, Kurs *et al.* Kurs et al. (2007) exploit the resonant magnetic technique to transfer energy from one storage device to another without any plugs or wires. The reported experiment demonstrated a wireless illumination of a 60 W light bulb from 2 meters away and achieved a 40% energy transfer efficiency. Zhang *et al.* Zhang et al. (2009) apply this technique to replenish battery energy in medical sensors and implantable devices in health care industry. Products from Powercast Powercast () carry out wireless charging by leveraging the electromagnetic radiation technique, with which energy transmitters broadcast the RF energy and receivers capture the energy and convert it to DC. Applications of the electromagnetic radiation technique for wireless charging have been reported in Tong et al. (2010); Li et al. (2010); Peng et al. (2010); He et al. (2011). As more and more applications of wireless charging technology have been envisioned, the Wireless Power Consortium WirelessPowerConsortium () has recently been established to start the efforts of setting an international standard for interoperable wireless charging.

The application of wireless charging technology to sensor networks is still in its infancy stage. Peng *et al.* Peng et al. (2010) recently study the feasibility of using the wireless charging technology to prolong the sensor network lifetime in a prototype system. The key idea is to dispatch a mobile robot to move around the network and charge energy to a selected set of lifetime-bottleneck sensor nodes. As the protocols run by sensor nodes should be simple and localized, the system employs two well-known routing protocols, i.e., energy-balanced routing and energy-minimum routing, both unaware of wireless charging activities. The charging strategy adopted by the system is simply to charge nodes with the lowest residual nodal lifetime. Hence, the wireless charger only passively makes up for the energy deficiency in the bottleneck nodes caused by the routing activities; that is, the charging activities are passively affected

by the routing activities. This may result in the following undesired consequences. If energy-minimum routing is used, nodes on the intersection of multiple energy-minimum routes may be overused even though the charger keeps charging them. When the energy consumption rates of these nodes exceed the charging capability, they deplete their energy quickly and the extension in the network lifetime is limited. Alternatively, if energy-balanced routing is used, the overall energy consumption in the network is increased as routes with longer length (and hence higher energy consumption) are used to bypass low-energy nodes which are on shorter and more energy-efficient routes. Hence, the energy replenished into the network may not be utilized efficiently.

In another recently reported effort, Shi *et al.* Shi et al. (2011) conduct theoretical study on efficient usage of the wireless charging technology in sensor networks. Based on the assumptions that the wireless charging capability is high enough to maintain an eternal network lifetime, the traffic pattern is fixed and the communication channels are perfect, they formulate and solve the problem of maximizing the ratio of the wireless charging vehicle's vacation time over each renewable energy cycle. Their solution is a static, centralized joint routing and charging algorithm. Hence, it may not be practical when the charging capability is constrained, the link qualities are imperfect and time-varying or the nodal energy consumption rates are heterogeneous and time-varying.

CHAPTER 3. Joint Routing and Charging Scheme

The key idea of J-RoC aims to employ energy-balanced routing and energy-minimum routing in a balanced way to exploit their strengths while avoiding or mitigating the problems caused by using only one of them. For this purpose, J-RoC requires periodical information exchanges between sensor nodes and the charger. Based on the exchanges, the charger keeps track of the global energy status of the network, schedules its charging activities accordingly, and disseminates the charging schedule to the network. Meanwhile, sensor nodes use a carefully designed *charging-aware* routing metric to estimate their routing costs and make routing decisions; this way, sensor nodes are guided to balance between energy-balanced routing and energy-minimum routing while the protocols run by them remain simple and localized.

3.1 Preliminaries

As illustrated in Figure 3.1, we consider a system composed of three main components: a mobile charger (MC) that is a mobile robot carrying a wireless power charger, a network of sensor nodes each equipped with a wireless power receiver, and a base station (BS) that monitors the energy status of the network and directs the MC to charge sensor nodes.

The system works as follows. Each sensor node generates sensory data and sends the data hop-by-hop to the sink periodically. It also measures its local energy level, monitors the channel conditions, estimates its energy consumption rate, and reports these information along with the data packet generation rate to the BS. Based on the collected information, the BS schedules future charging activities, and commands the MC via a long range radio to execute the schedule. The MC then travels around the deployment field to charge sensor nodes. The BS also disseminates the schedule to sensor nodes, which may be used in routing path construction.

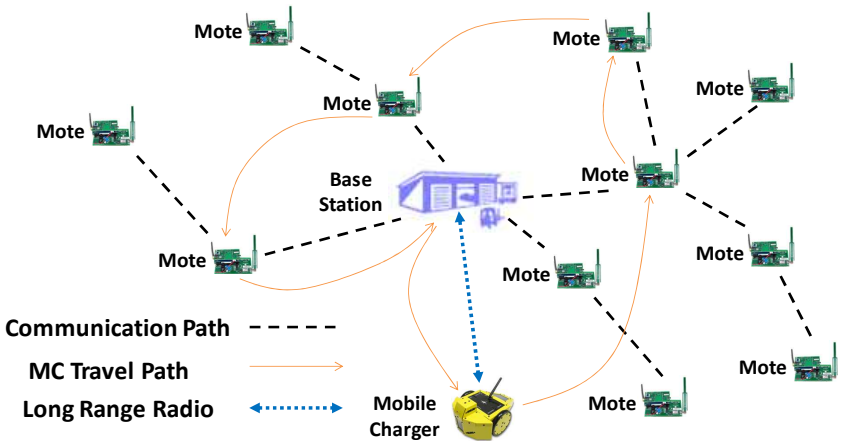

Figure 3.1 System Overview.

We assume the MC's energy can be replenished at the BS and thus the energy for moving and charging is unlimited.

Notations used in this thesis are listed in Table 3.1.

3.2 J-RoC: A Joint Routing and Charging Scheme

In this section, we present J-RoC – a Joint Routing and Charging scheme. As shown in Figure 3.2, J-RoC works through periodical interactions between the sensor nodes, the base station (BS) and the mobile charger (MC).

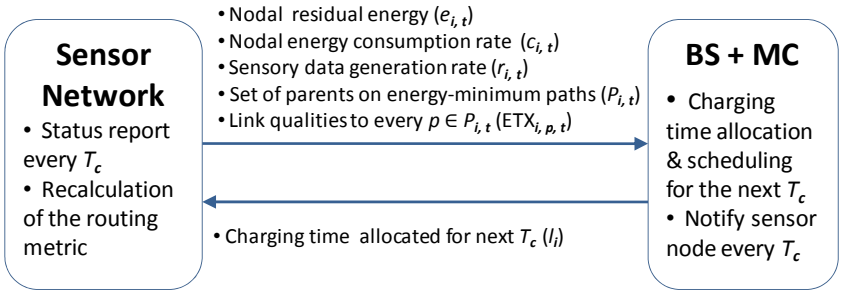

Figure 3.2 Overview of the proposed J-RoC scheme.

Every T_c time, the BS determines a charging schedule (i.e., charging time l_i for each sensor node i) for the next T_c interval. As detailed in Section 3.2.2, the schedule is decided based on the

Table 3.1 Notations Used in the Joint Routing and Charging Problem

notation	meaning
E_s	battery capacity of a sensor node
e_{tx}	energy consumed for transmitting a packet
e_{rx}	energy consumed for receiving a packet
Λ_c	energy consumed for the MC's charging operation
η	MC's charging efficiency
v	MC's moving speed
T_c	charging activity scheduling interval
α	charging guiding coefficient
l_i	charging time allocated to node i in one T_c interval
$r_{i,t}$	future sensory data packet generation rate of node i estimated at time t
$\varphi_{i,t}$	amount of time that node i has been charged in the current T_c interval at time t
$h_{i,t}$	charging rate of node i at time t
$e_{i,t}$	residual energy of node i at time t
$c_{i,t}$	energy consumption rate of node i at time t
$c'_{i,t}$	energy consumption rate of node i at time t in transceiving via the energy-minimum routing paths
$\hat{c}_{i,t}$	future energy consumption rate of node i estimated at time t
$P_{i,t}$	set of node i's parents on the energy-minimum path at time t
$ETX_{i,j,t}$	expected number of transmissions needed to send a packet successfully from node i to j at time t
ρ_i	percentage of charging energy that should be allocated to node i in one T_c interval

following information reported by each node: its energy consumption rate, residual energy level, data packet generation rate, set of parents on the energy-minimum paths to the sink, and the qualities of links to each parent. The BS disseminates the schedule to nodes and commands the MC to execute it. To reduce the control message overhead incurred by the periodical interactions between the BS and the network, the interaction interval can be configured to be much larger than the sensor data report interval. This will not compromise the system performance much, because the status of the network likely will not change significantly until a relatively large amount of data have been transmitted and received. For example, the data report interval is 2.5 seconds in our testbed experiments, and we set the interaction interval to be one hour. Evaluation results in Section 4.1 show that such a configuration performs well

and yields a network lifetime that is reasonably close to the upper bound.

The Collection Tree Protocol (CTP) Gnawali et al. (2009) is used as the routing protocol in J-RoC to report sensory data and nodal status to the BS. CTP is the default routing protocol in TinyOS 2.x. It designates a node in the network as the sink node. All other nodes recursively form routing trees rooted at the sink. Nodes periodically broadcast beacons which serve two purposes. Firstly, they contain a field that the link estimator component of TinyOS uses to estimate the expected number of transmissions needed to send a packet successfully (ETX) to a node's neighbor, which roughly reflects the reciprocal of the packet reception ratio ($\frac{1}{PRR}$) over the link. Secondly, nodes embed in these beacons an estimate of the total cost (zero for the sink node and ∞ for others, initially) of routing a data packet to the sink from them. Non-sink nodes then collect the advertised routing costs from their neighbors, add their own one-hop routing costs, and select the neighbors with the lowest total routing costs as their parents. Since the beacons are broadcasted periodically, nodes can dynamically change their parents as routing costs fluctuate.

In J-RoC, each sensor node embeds two types of routing costs in CTP beacons. One contains the total cost of routing a packet to the sink along a charging-aware path. The other one contains the cost of delivering a packet along the energy-minimum path. Here, the energy-minimum path is defined as the path with the minimum total energy consumption in delivering a packet from a source to a destination. Link quality has been considered in estimating the energy consumption. In J-RoC, all data packets are routed via the aforementioned charging-aware paths to the sink. Note that the paths are different from the conventional energy-balanced or energy-minimum ones; as to be elaborated, the selection of the paths considers simultaneously the effects of energy charging, energy balancing and energy efficiency.

3.2.1 Routing Cost

After receiving the costs from neighbor nodes, sensor node i calculates its *energy-minimum* routing cost ($\mathcal{C}'_i$) as follows:

$$\mathcal{C}'_i = \min_{j \in N_i} \left\{ \mathcal{C}'_j + ETX_{i,j,t} \right\}, \tag{3.1}$$

where N_i is the set of node i's neighbor nodes, $\mathcal{C}'_j$ is the routing cost of node j and $ETX_{i,j,t}$ represents the expected number of transmissions needed to send a packet successfully over link (i, j). Hence, Equation (3.1) computes the minimum number of transmissions needed to deliver a packet from i to the sink successfully. Note that when links are in perfect condition, e.g., $ETX_{i,j,t} = 1$ for any i and j, the energy-minimum path becomes the shortest path.

The *charging-aware* routing cost at node i ($\mathcal{C}_i$) is computed as follows:

$$\mathcal{C}_i = \min_{j \in N_i} \left\{ \mathcal{C}_j + u^{1-\frac{\hat{e}_{i,j,t}}{E_s}} \right\}, \tag{3.2}$$

where $\mathcal{C}_i$ is the routing cost of node j, E_s is the battery capacity of a sensor node, and $\hat{e}_{i,j,t}$ in routing metric $u^{1-\frac{\hat{e}_{i,j,t}}{E_s}}$ is computed as

$$e_{i,t} + (l_i - \varphi_{i,t})\Lambda_c \eta - t_r * c_{i,\hat{p}_{i,t},t} * \frac{ETX_{i,j,t}}{ETX_{i,\hat{p}_{i,t},t}}. \tag{3.3}$$

In Equation (3.3), $\varphi_{i,t}$ denotes how long node i has been charged in the current T_c interval, t_r represents the remaining time in the current T_c interval and $\hat{p}_{i,t}$ denotes the parent of node i on the charging-aware path at time t. The term $c_{i,\hat{p}_{i,t},t} * \frac{ETX_{i,j,t}}{ETX_{i,\hat{p}_{i,t},t}}$ estimates the nodal energy consumption rate if i switches its parent from $\hat{p}_{i,t}$ to j. As the nodal energy consumption rate $c_{i,t}$ is measured when $\hat{p}_{i,t}$ is i's parent, we abbreviate $c_{i,\hat{p}_{i,t},t}$ to $c_{i,t}$ in the following sections.

The purpose of using this routing cost is to balance the energy consumption in the possibly lossy wireless environment among sensor nodes in the presence of energy charging. If there is no energy charging, a well-known energy-balanced routing metric Kar et al. (2003) is

$$u^{1-\frac{e_{i,t}}{E_s}}. \tag{3.4}$$

Though the energy-balanced routing extends the network lifetime, different approaches should be adopted when energy charging is available. With energy charging, as much as possible energy should be replenished into nodes on the energy-minimum paths, so that these nodes can live longer and allow others to use them for packet routing, which can improve the energy utilization efficiency and hence prolong the network lifetime. However, as charging takes long time to be accomplished, nodes selected to be charged may not often maintain a high residual energy level, and therefore, energy-minimum paths may not often be chosen by other nodes to

route their packets if Equation (3.4) is used to compute the routing cost. Furthermore, in some environments, particularly in the 2.4 GHz frequency band, links could be highly lossy Srinivasan et al. (2008). Without the knowledge of the link quality, lots of energy may be wasted on packet retransmissions over lossy links.

Our proposed routing metric addresses the above problems by factoring in the effects of charging that has been planed but not executed yet to estimate the routing cost, as well as the real-time link quality. Specifically, $\hat{e}_{i,j,t}$ estimates node i's residual energy at the end of the current T_c interval when it selects node j as parent, based on the knowledge of the charging schedule and link quality as in Equation (3.3). Then, $\hat{e}_{i,j,t}$ instead of $e_{i,t}$ is used in the routing metric as in Equation (3.2). Hence, nodes are led to choose paths to balance their residual energy at the end of the current T_c.

Figure 3.3 demonstrates how $\hat{e}_{i,j,t}$ is estimated at time $t = t_{curr}$. Note that, in this example, the energy consumption rate of node i is assumed to be constant from the current time to the end of the T_c interval to simplify the estimation. Specifically, in Figure 3.3, $c_{i,t_{curr}}, e_{i,t_{curr}}, h_{i,t_{curr}}$ are the energy consumption rate, nodal residual energy and charging rate at time t_{curr}, respectively. $\varphi_{i,t_{curr}}$ is the amount of time that node i has been charged in this T_c interval, l_i is the amount of charging time allocated to node i in this T_c interval and $l_i - \varphi_{i,t_{curr}}$ is the amount of remaining charging time. Assuming the future energy consumption rate does not change, Equation (3.3) estimates the residual nodal energy at time $(n+1)T_c$.

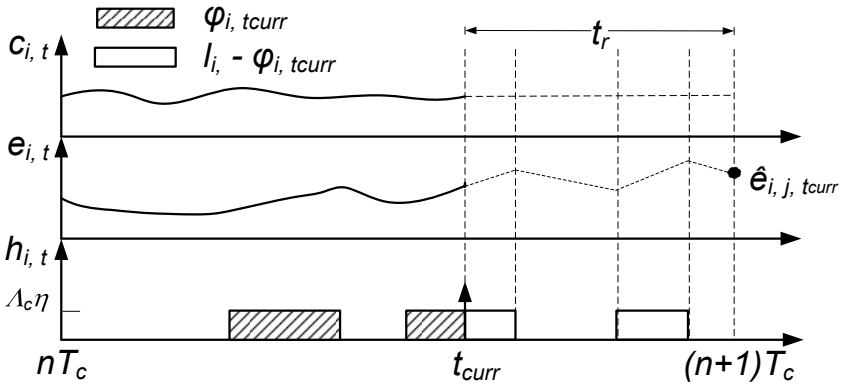

Figure 3.3 Computation of $\hat{e}_{i,j,t}$.

3.2.2 Charging Scheduling Algorithm

Every T_c time, sensor nodes report their nodal status to the BS, including residual energy level ($e_{i,t}$), energy consumption rate ($c_{i,t}$), sensory data packet generation rate ($r_{i,t}$), set of parents on the energy-minimum paths to the sink ($P_{i,t}$), and the expected number of transmissions to deliver a packet successfully to each parent $p \in P_{i,t}$ ($ETX_{i,p,t}$), based on which the BS schedules the charging activities for the next T_c interval. t is the time when node i reports these information to the BS. The charging scheduling algorithm works in two phases. Firstly, it selects a set of sensor nodes that should be charged in the next T_c interval. Secondly, it determines a sequence in which the sensor nodes are charged so that the movement time is minimized. It also distributes the amount of charging time l_i for the next T_c interval to each node in the sequence.

3.2.2.1 Charging Energy Allocation

To allocate charging energy to sensor nodes, the BS first estimates the future nodal energy consumption rate, denoted as $\hat{c}_{i,t}$, for every sensor node i. Let ρ_i be the percentage of charging energy that should be allocated to sensor node i in one T_c interval. To maximize the network lifetime is to maximize

$$\min_i \left\{ \frac{e_{i,t}}{\hat{c}_{i,t} - \rho_i * \Lambda_c * \eta} \right\}, \tag{3.5}$$

where $0 \leq \rho_i \leq 1$ and $\sum_i \rho_i \leq 1$. Algorithm 1 applies the binary search method to solve the optimization problem.

Next, we discuss how to estimate $\hat{c}_{i,t}$. For a sensor network without energy charging, the energy-balanced routing is favored to extend the network lifetime. The strategy, however, has a side-effect that packets may be routed through less energy efficient paths to the sink when the energy-minimum paths have nodes with low residual energy. Hence, compared to the energy-minimum routing, the energy-balanced routing consumes more energy in transmitting packets. In a sensor network with wireless charging, the MC is able to charge the energy bottleneck nodes. Therefore, energy-minimum paths should be employed more often to improve the energy utilization efficiency in communication and thus to elongate the network lifetime. Based on

Algorithm 1 Charging scheduling algorithm to maximize the minimal nodal lifetime

Input: $e_{i,t}$ and $\hat{c}_{i,t}$ for every sensor node i
Output: ρ_i

1: $low \leftarrow \min \frac{e_{i,t}}{\hat{c}_{i,t}}, up \leftarrow \infty$
   /* *low/up is the lower/upper bound of the network lifetime* */
2: $target \leftarrow low$
   /* *target is the maximum achievable network lifetime* */
3: **while** $up - low > \epsilon$ **do**
4: calculate ρ_i by solving $target = \frac{e_{i,t}}{\hat{c}_{i,t} - \rho_i * \Lambda_c * \eta}, \forall i \in V$
5: **if** $\sum_{i,\rho_i>0} \rho_i > 1$ **then**
6: $up \leftarrow target$
7: $target \leftarrow \frac{low+up}{2}$
8: **else**
9: $low \leftarrow target$
10: $target \leftarrow (up = \infty)?2 * low : \frac{low+up}{2}$
11: return ρ_i

this observation, the proposed charging scheduling algorithm should intentionally allocate more energy to nodes on energy-minimum paths in order to guide sensor nodes to utilize these paths more frequently. For this purpose, $\hat{c}_{i,t}$ is computed as

$$\hat{c}_{i,t} = \alpha c'_{i,t} + (1 - \alpha) c_{i,t}, \tag{3.6}$$

where $c_{i,t}$ is the actual energy consumption rate reported by node i, $c'_{i,t}$ is the energy consumption rate of node i if all sensor nodes use energy-minimum paths, and α is a value between 0 and 1, called the charging guiding coefficient. In the following, we present how to determine $c'_{i,t}$ and α.

Based on the collected $P_{i,t}$ information from each sensor node, the BS can build a directed acyclic graph. Note that, if sensor node i has multiple energy-minimum paths towards the sink (e.g., several paths from i have the same value of Equation (3.1)), we assume that it transmits packets evenly among these paths. Specifically, if i has k energy-minimum paths, it embeds all k energy-minimum parents and the corresponding link qualities to each parent in the status report to sink. As link qualities are usually stable in a relatively long run Zhao and Govindan (2003), we assume that the energy-minimum paths do not change much during one T_c interval as long as T_c value is in a reasonable range. Suppose each sensor node generates a packet at

rate $r_{i,t}$ in future, and all sensor nodes use energy-minimum paths to transmit packets. To transmit the packets for itself, the energy consumption rate at sensor node i is

$$\sum_{s \in S_{i,t}} e_{tx} * ETX_{i,n^s_{i,t},t} * \frac{r_{i,t}}{|S_{i,t}|}, \tag{3.7}$$

where $S_{i,t}$ denotes the set of energy-minimum paths from sensor node i to the sink and $n^s_{i,t}$ denotes the next hop node of i on the energy-minimum path s. To successfully forward packets generated by other nodes, the energy consumption rate at i is

$$\sum_{j \neq i} \sum_{s \in S_{j,t}} (e_{rx} * ETX_{b^s_{i,t},i,t} + e_{tx} * ETX_{i,n^s_{i,t},t}) * \frac{r_{j,t}}{|S_{j,t}|} * I_{i \in s}, \tag{3.8}$$

where $I_{i \in s}$ is an indicator function whose value is 1 if and only if node i is on path s and $b^s_{i,t}$ denotes the previous hop node of i on the energy-minimum path s. e_{tx} and e_{rx} are the expected energy consumed to transmit and receive a packet, respectively, and the values depend on the specific underlying MAC protocols. Hence, $c'_{i,t}$ can be computed by summing up Equation (3.7) and Equation (3.8). Figure 3.4 shows an example of the above procedure. Suppose $\forall i, j, r_{i,t} =$ 1 pkt/s, $e_{tx} = e_{rx} = 0.06$ J/pkt and $ETX_{i,j,t} = 1$ except $ETX_{3,sink,t} = 3$ and $ETX_{1,sink,t} = 2$. (a) shows the topology of a network with 10 source nodes and the black square represents the sink. (b) shows the $c'_{i,t}$ value for each node. All routing paths connecting the sensor nodes and the sink are the energy-minimum ones. As node 4 needs two transmissions to reach the sink while node 3 needs three transmissions, path $6 \rightarrow 4 \rightarrow 2$ is the energy-minimum path. Take node 4 for instance; for each of the nodes 7, 8, 9, and 10, it has three energy-minimum paths to the sink and two of them pass through node 4; for node 5, it has two energy-minimum paths to the sink and only one of them passes through node 4; for node 6, it only has one energy-minimum path to the sink and it passes through node 4. Therefore, the energy consumption rate for node 4 to relay the packets for nodes 5, 6, 7, 8, 9 and 10 is $(\frac{2}{3} * 4 + \frac{1}{2} + 1) * (0.06 + 0.06) = 0.5$ J/s, the energy consumption rate for transmitting its own packets is 0.06 J/s; hence we have $c'_{4,t} = 0.56$ J/s.

The value of the charging guiding coefficient α is related to two factors. One factor is the relative charging capability of the MC, which is reflected by the ratio between the amount of energy that can be charged per time unit (i.e., $\Lambda_c * \eta$) and the whole network energy consumption

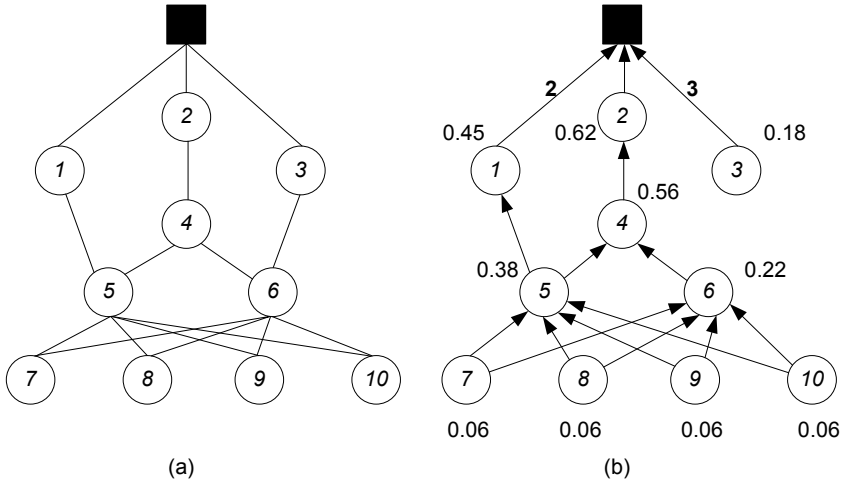

Figure 3.4 An example of calculating $c'_{i,t}$ values.

rate (i.e., $\sum_i c_{i,t}$). When the charging capability is relatively strong, e.g., $\frac{\Lambda_c * \eta}{\sum_i c_{i,t}}$ is large, a larger α values is favorable. This means that the charging scheme should guide more packets to be delivered along the energy-minimum paths as the capability of the MC is strong enough to compensate the energy deficiency in time, and accordingly, more energy should be allocated to nodes on the energy-minimum paths. When the capability is low, a smaller α value should be used instead. In addition, the u value also affects the allocation of the chargeable energy. When $u = 1$, each sensor node uses a fixed shortest path to route packets, and therefore is not affected by the charging schedule. When $u > 1$, each sensor node selects its path based on the routing metric. As the routing metric in Equation (3.2) is affected by the charging schedule, the routing decision can be guided by adjusting the charging schedule. Besides, the larger is u, the more effective is the guidance. Considering both factors, we define α as:

$$\alpha = 1 - u^{-\frac{\Lambda_c * \eta}{\sum_i c_{i,t}}}. \tag{3.9}$$

With this formula, when $u = 1$, α is equal to 0 and $c'_{i,t}$ has no impact on the consumption rate estimation. When $u > 1$, the stronger is the relative charging capability, the larger is α and the more weight is given to $c'_{i,t}$ when computing $\hat{c}_{i,t}$.

3.2.2.2 Charging Sequence Determination

In practice, the moving speed of a robot is limited Dantu et al. (2005) (e.g., between 0.2 and 2 m/s). Too frequent movement may waste time that can be used to charge sensor nodes. Hence, given an allocation plan of charging energy, as computed above, it is important to determine a charging sequence to implement the allocation with as little movement as possible.

The procedure of the charging sequence determination works as follows and an example is given in Figure 3.5. Figure 3.5(a) shows the positions of 5 nodes and triangle 0 stands for the MC. Figure 3.5(b) gives a naive charging sequence where the MC visits the nodes in the ascending order of nodal lifetime $\frac{e_{i,t}}{\hat{c}_{i,t}}$. The shadow width represents the moving time. Figure 3.5(c) shows the procedure of merging ρ_1 and ρ_4 into ρ_2. Figure 3.5(d) shows the final charging sequence rearranged by the VRPTW solver.

- Given the percentage of the charging energy ρ_i, the sensor nodes are sorted ascendingly according to their nodal lifetime $\frac{e_{i,t}}{\hat{c}_{i,t}}$. For example, Figure 3.5(a) illustrates the position and nodal lifetime of 5 nodes where the e_i values are 750, 300, 150, 750, 900 J and the $\hat{c}_{i,t}$ values are 0.015, 0.02, 0.03, 0.015, 0.01 J/s. The output of Algorithm 1 produces ρ_i values as 4%, 32%, 60%, 4%, 0% and *target* as 55714 s assuming $\Lambda_c\eta = 0.045$ J/s. Figure 3.5(b) shows the sorting result. It also gives us a naive charging sequence with possibly high movement overhead, e.g, $T_e = T_c - T_m^{0,3,2,1,4}$ where $T_m^{0,3,2,1,4}$ is the total moving time along the trajectory $0 \to 3 \to 2 \to 1 \to 4$ and T_e is the effective charging time. $\rho_i * T_e$ is the amount of charging time allocated to node i.

- The ρ_i value of the maximum lifetime node is iteratively merged to that of the minimum lifetime node until the the battery ceiling of the minimum lifetime node is reached, i.e., $\frac{E_s - e_{i,t}}{\Lambda_c\eta} < \rho_i * T_e$. For example, in Figure 3.5(c), ρ_4 is merged into ρ_3 at first. If the updated ρ_3 does not result in a battery ceiling hit, we update $T_e = T_c - T_m^{0,3,2,1}$ and $\rho_3 = \rho_3 + \rho_4$. Then, the algorithm tends to merge ρ_1 into ρ_3. If the merging leads to a battery ceiling hit, we merge a part of ρ_1 value into ρ_2. This procedure ends when the maximum nodal lifetime is less than T_c or only one node exists after merging.

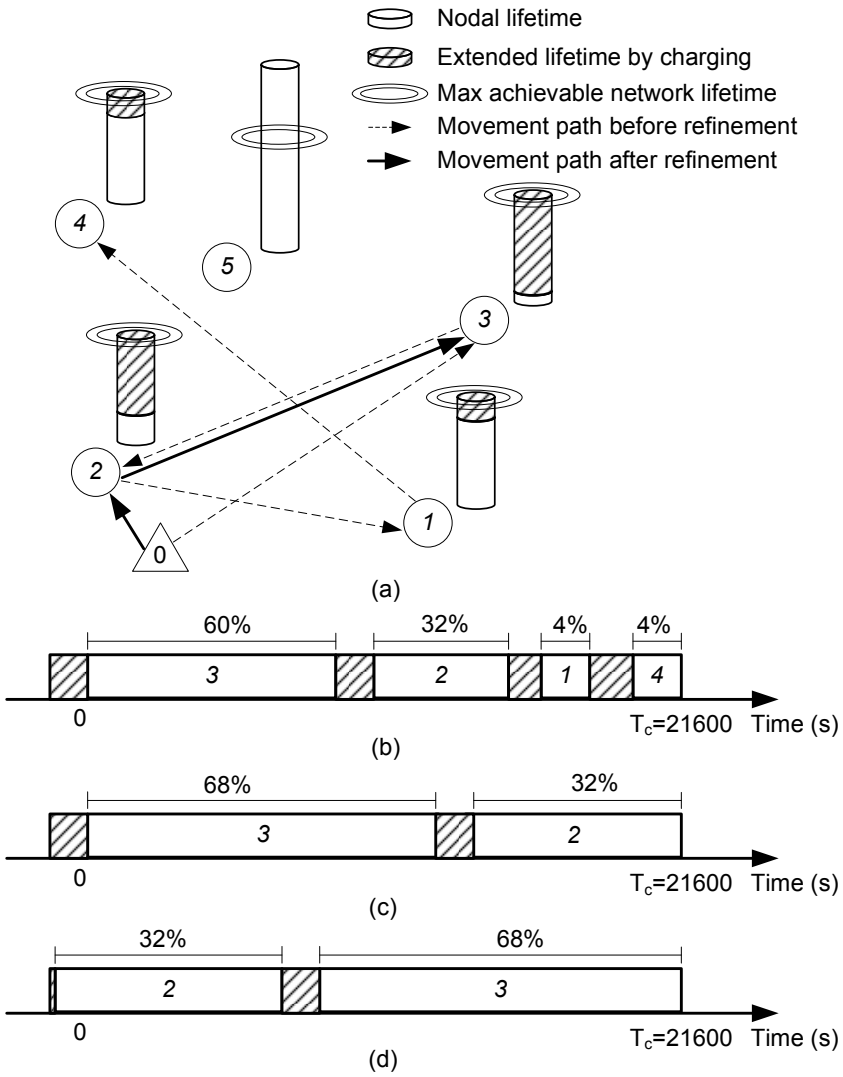

Figure 3.5 An example of the movement refinement.

- VRPTW solver JOpt.NET (), which solves the vehicle routing problem with time window Lenstra and Kan (1981), is called to rearrange the visiting sequence to further reduce the movement time. Here, the nodal lifetime is the deadline for each node to be visited. For example, in Figure 3.5(d), the rearranged sequence has $T_m^{0,2,3} < T_m^{0,3,2}$ and $T_e = T_c - T_m^{0,2,3}$. $\rho_i * T_e$ is the amount of charging time allocated to node i and the final charging sequence ready for execution is $\langle\langle 2, \rho_2 T_e\rangle, \langle 3, \rho_3 T_e\rangle\rangle$. Obviously, the amount of effective charging time after the movement refinement is much larger than the one before and thus more energy is replenished into the network.

3.2.3 Performance Upper Bound

Here, we assume the sensory data packet generation rate $r_{i,t}$ of a node does not change during the network lifetime and thus $r_{i,t}$ is denoted as r_i. When the MC's movement delay is ignored and the link qualities are perfect, the optimal solution can be described by the following linear programming formulation.

$$\max \quad T,$$

s.t.:

$$T * r_i + \sum_{j \in N_i} f_{j,i} = \sum_{j \in N_i} f_{i,j}, \tag{3.10}$$

$$T * \sum_i r_i = \sum_{j \in N_{BS}} f_{j,BS}, \tag{3.11}$$

$$e_{tx} * \sum_{j \in N_i} f_{i,j} + e_{rx} * \sum_{j \in N_i} f_{j,i} \leq E_s + a_i * \Lambda_c * \eta, \tag{3.12}$$

$$\sum_i a_i \leq T, \tag{3.13}$$

$$f_{i,j}, a_i \geq 0. \tag{3.14}$$

Here, T is the network lifetime. $f_{i,j}$ is the total number of packets transmitted from nodes i to j during the network lifetime. a_i is the total amount of time that the MC charges i.

Constraints (3.10) and (3.11) reflect the flow conservation requirements. Constraint (3.12) reflects that the energy used for transmission and reception should be smaller than E_s – the battery capacity of a sensor node – plus the energy charged from the MC. Constraint (3.13) states that the MC could charge one node at a time and thus the total charging time cannot exceed the network lifetime. The output $\langle f_{i,j}, a_i \rangle$ is the joint routing and charging solution. It specifies the number of data packets transmitted over the link (i, j) and the total charging time on node i so that the network lifetime can be maximized.

However, the LP formulation does not take the MC's movement and packet retransmissions into account. Hence, it provides an upper bound of the achievable network lifetime. This

formulation is used in both testbed experiment and simulation to evaluate the performance of the proposed J-RoC scheme.

3.3 Design and Implementation

To evaluate the performance of the proposed J-RoC scheme, we have built a prototype system, and the design details of this system are as follows.

3.3.1 Hardware Component

In the prototype system, a Powercast wireless power charger Powercast () is installed on an Acroname Garcia robot Garcia () which works as the MC, and a Powercast wireless power receiver is connected to the batteries of a sensor node. The MC communicates with the BS (a PC in the experiments) via an IEEE 802.11b interface to receive the charging scheduling information. When the MC moves into close proximity of a sensor node, the power receiver can collect the energy transferred wirelessly from the MC and use it to charge the batteries of the node.

The energy charging is carried out in the 903-927 MHz band while sensor nodes communicate in the 2.4 GHz band. The power consumption is 3 W when the MC is charging, and the effective amount of energy that can be captured by a receiver varies with the distance between the receiver and the MC; that is, the charging efficiency decreases exponentially when the distance increases. In our system, the MC moves at 1 m/s and the average distance between it and the node charged is about 10 cm which results in 45 mW received power. Note that we use the Powercast products only to evaluate J-RoC's performance in our prototype system.

3.3.2 Software Component

Figure 3.6 shows the software architecture where the shaded parts were elaborated in Section 3.2. The software running on the base station is developed in JAVA, and the sensor node software is developed based on TinyOS 2.1.

In the node software, the *routing engine* module periodically broadcasts beacons containing the information about the energy-minimum path cost and the current routing path cost from

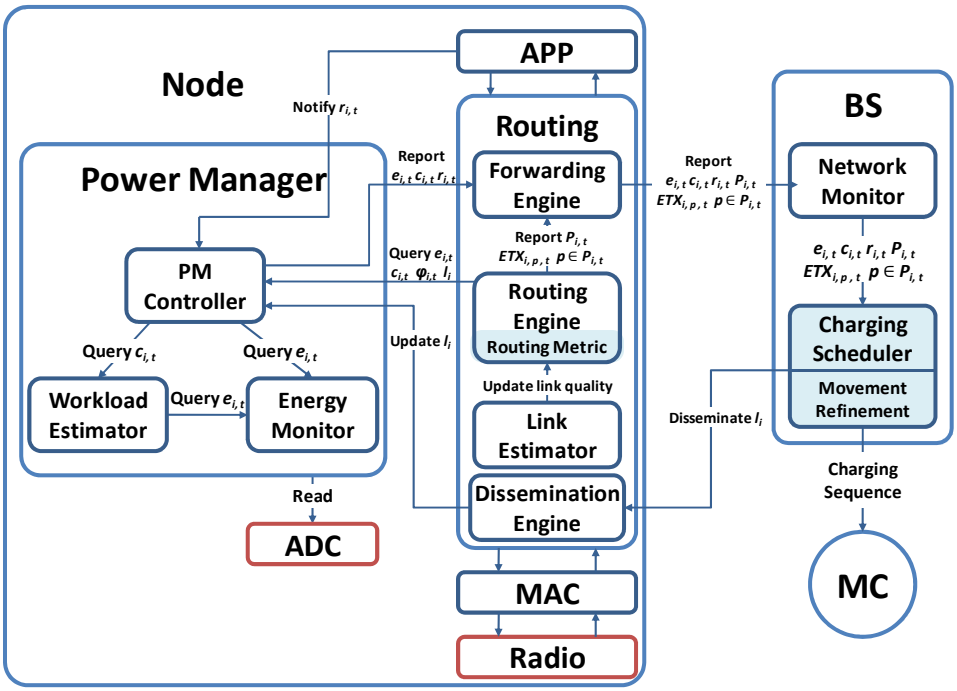

Figure 3.6 Conceptual sketch of the software component.

the node to the BS. The costs are computed using Equations (3.1) and (3.2) respectively with the latest information of $c_{i,t}, e_{i,t}, \varphi_{i,t}$ and l_i from the *power manager* component and $ETX_{i,j,t}$ from the *link estimator* module. Once receiving a beacon, a node selects the neighbor with the least routing cost to be its next-hop node and updates the energy-minimum parent. The *forwarding engine* module is responsible for forwarding the sensor data packets for the *application* component, and the status reports for the power manager component. The *dissemination engine* module informs the power manager component of the latest l_i value when it receives the charging scheduling messages from the BS. The application component notifies the power manager component of the future sensory data packet generation rate $r_{i,t}$.

The power manager component boots up automatically with the system and maintains all the charging and nodal energy related information. The *power controller* module records the elapsed charging time $\varphi_{i,t}$ during a T_c interval. It also reports the latest nodal residual energy $e_{i,t}$ (provided by the *energy monitor* module), the energy consumption rate $c_{i,t}$ (provided by the *workload estimator* module) and the $r_{i,t}$ value, together with the $P_{i,t}$ and $ETX_{i,p,t}, p \in$

$P_{i,t}$ (provided by the *routing engine* module) to the BS periodically. In our implementation, the workload estimator module employs the exponentially weighted moving average (EWMA) method to estimate the $c_{i,t}$ values.

At the BS, after the energy reports from each node have been received, the *network monitor* component updates $e_{i,t}$, $c_{i,t}$, $r_{i,t}$, $P_{i,t}$ and $ETX_{i,p,t}, p \in P_{i,t}$ of a node accordingly in a timely manner. Every T_c interval, new charging activities are determined by the *charging scheduler* component with the algorithm described in Section 3.2.2; then, the BS informs the MC of the new schedule and disseminates the messages containing the latest l_i value to the network.

CHAPTER 4. Evaluation

4.1 Experimental Study

4.1.1 Experimental Setup

In the experiments, 10 TelosB sensor nodes are deployed according to the topology shown in Figure 3.4(a). The neighboring nodes are two meters apart and the CC2420 radio transmission power is set to level 3 which results in a 3.5 m communication range. The sink node is connected to a PC with stable power supply and does not need to be charged. During the experiments, each sensor node generates a data packet every 2.5 seconds. A modified X-MAC Buettner et al. (2006) protocol is run on each sensor node with a Low Power Listening interval of 250 ms and default channel checking time of 50 ms. The T_c length is one hour to reschedule the charging activities.

Each sensor node is powered by two 1.5 V 2000 mAh alkaline rechargeable batteries, and Figure 4.1 shows the mapping between the residual energy and battery voltage level. Particularly, 3000 J energy is consumed in the voltage range 3 V$\sim$2.6 V with running time of 8.4 hours, 7000 J is consumed in the voltage range 2.6 V$\sim$2.2 V in a slower pace with 23 hour running time and 2000 J is consumed in the voltage range 2.2 V$\sim$1.9 V with 5.3 hour running time. The running time is measured with 100% radio duty cycle. The result is achieved through five trials of experiments with 100% radio duty cycle.

To save experiment time, the evaluation is conducted when the voltage varies from 3 V to 2.6 V in which range more serious battery leakage is accompanied as illustrated in Figure 4.1. For each node, the energy level is 100% when the voltage reading is 3 V and the battery is assumed to be completely depleted at voltage level 2.6 V.

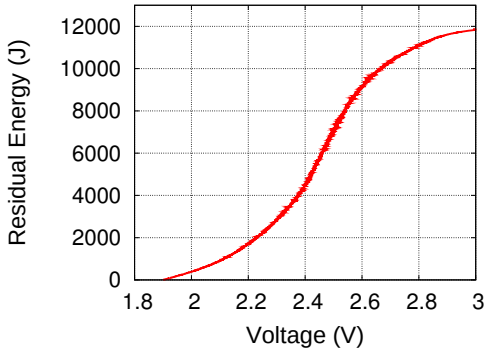

Figure 4.1 Battery energy profile.

4.1.2 Evaluation Results

In the experiments, we evaluate (i) the network lifetime upper bound according to 3.2.3 and the actually achieved network and nodal lifetime, when the energy-balanced routing is used without charging (tagged as *no charge* in the figures), the energy-balanced routing combined with greedyPlus scheme Peng et al. (2010) is used, and the J-RoC scheme is used, respectively; (ii) the average packet rate (including both the self-generated and the forwarded data packets) of individual nodes; and (iii) the distribution of charging time to individual nodes. As simulation results in Peng et al. (2010) have shown that greedyPlus scheme performs better with energy-balanced routing than with energy-minimum routing, we only show the results of greedyPlus with energy-balanced routing in the experiment and simulation evaluations. Parameter u is set to 1000.

4.1.2.1 Overall Evaluation Result of J-RoC

Figure 4.2(a) shows the network lifetime upper bound and the nodal lifetime of individual nodes. The network lifetime upper bound is 30 hours while the achieved network lifetime is 14.9 hours (bounded by node 3), 20.5 hours (bounded by node 5) and 25.5 hours (bounded by node 1) for no charge, greedyPlus and J-RoC respectively. The advantage of J-RoC on prolonging the network lifetime is demonstrated in two aspects in the figure. First of all, compared to the no charge case, the ratio of network lifetime improvement is about 71% (from 14.9 hours to 25.5 hours); compared to the greedyPlus scheme, the ratio of improvement is about 24%

(from 20.5 hours to 25.5 hours). Moreover, J-RoC achieves 85% of the network lifetime upper bound (25.5 hours out of 30 hours). Secondly, the J-RoC scheme helps to reduce the standard deviation of the nodal lifetime which results in more efficient usage of the energy. Specifically, the standard deviation of the nodal lifetime is 6.6 hours for J-RoC, 8.6 hours for greedyPlus and 12.3 hours when there is no energy charging.

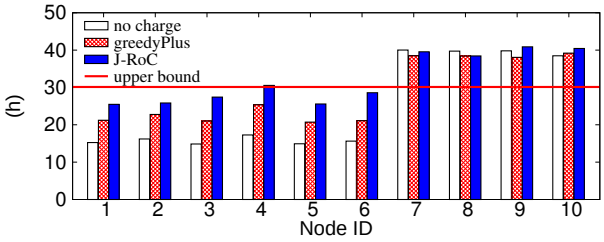

(a) Lifetime of network and individual nodes.

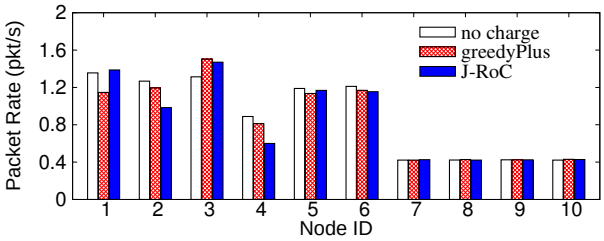

(b) Average data packet rate in individual nodes.

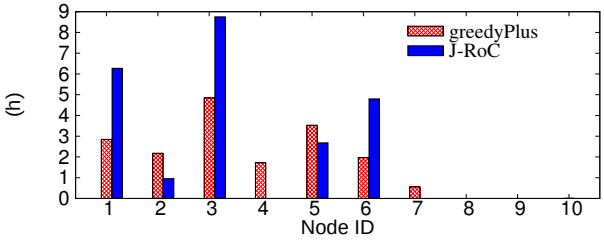

(c) Distribution of charging time among sensor nodes.

Figure 4.2 Experimental results.

The improvement in network lifetime shown by Figure 4.2(a) is achieved by guiding nodes to use energy-minimum paths more frequently and allocating more charging energy to nodes on these paths. The average packet rate shown in Figure 4.2(b) and the charging time allocation

depicted in Figure 4.2(c) reveal these behaviors in detail.

As shown by Figure 4.2(b), nodes 1, 2 and 3 have forwarded quite different numbers of packets when different schemes are used, though they are all one-hop away from the sink. With no charge, these nodes are equally used and their packet rates are all around 1.3 pkt/s because the energy-balanced routing is used. When J-RoC is used, node 2's packet rate drops to 0.95 pkt/s, which is significantly lower than the packet rates of nodes 1 and 3 (i.e., 1.45 pkt/s and 1.55 pkt/s, respectively). When the greedyPlus scheme is used, node 2's packet rate is approaching 1.3 pkt/s and the packet rate of node 3 is much higher than that of node 1 and node 2 respectively. Figure 4.2(c) shows that the charging patterns to nodes 2 and 4 are different when different schemes are used. With greedyPlus, both nodes 2 and 4 are charged with 4 hours in total, but only node 2 is charged in J-RoC and the charging time is less than 1 hour. These differences are attributed to the following reasons. First of all, in greedyPlus, the routing decisions are made without the knowledge of charging activities, and therefore, packets are routed in the energy-balanced manner by using paths through nodes 1, 2 and 3 evenly. The J-RoC scheme, on the other hand, tends to guide nodes to utilize the energy-minimum paths more frequently. Also, if a node has multiple energy-minimum paths that can be used, it is guided to use them in a balanced way. Hence, fewer packets go through node 2, more packets are forwarded by nodes 1 and 3, and the numbers of packets passing nodes 1 and 3 are similar. Secondly, the charging decisions made by greedyPlus is simply to balance nodal lifetimes, without considering routing activities in the network. Therefore, both nodes 2 and 4 are charged with a significant amount of energy as they consume a significant amount of energy to forward packets toward the sink. Differently, the J-RoC scheme makes charging decisions through considering two factors in a balanced manner: guiding nodes to use energy-minimum paths more often, and balancing nodal lifetimes. Consequently, nodes 2 and 4 are seldom charged as they are not on energy-minimum paths and they consume less energy to forward packets than nodes 1 and 3.

In general, the differences in the nodes' packet rates and the allocated charging time among individual nodes reveal the principle behind the design of the J-RoC scheme.

4.1.2.2 Summary

The experimental results have demonstrated the advantage of J-RoC on improving the network lifetime through proactively guiding the routing activities and delivering the energy to where it is needed. When J-RoC is used, more packets are routed through the energy-minimum paths and more charging energy is allocated to nodes on these paths.

4.2 Simulation Study

4.2.1 Simulation Setup

Extensive simulations have been conducted in a custom simulator to evaluate the performance of J-RoC in large-scale networks. In the simulations, 100 nodes are randomly deployed to a 500 m $\times$ 500 m field. The base station and the sink are placed in the center of the field. Table 4.1 lists the default simulation parameters. As the charging scheduling interval T_c is much larger than the data report interval (default 6 hours compared to 4 minutes), the overhead of the nodal status information collection and charging scheduling information dissemination is neglected in the simulation.

Table 4.1 Simulation Parameters

Parameter	Value
communication range of a sensor node (m)	70
battery capacity of a sensor node: E_s (KJ)	10
energy consumed for MC's charging operation: Λ_c (W)	3
energy consumed for transmitting a packet: e_{tx} (J/pkt)	0.05
energy consumed for receiving a packet: e_{rx} (J/pkt)	0.06
MC's charging efficiency: η (%)	1.5
MC's moving speed: v (m/s)	1
system parameter u	1000
data generation rate: r_i (pkt/h)	15
charging scheduling interval T_c (h)	6

4.2.2 Simulation Results

We measure the network lifetime achieved by the J-RoC scheme, the greedyPlus scheme Peng et al. (2010), and the upper bound network lifetime derived in Section 3.2.3 under different scenarios with varying T_c interval, routing metric parameter u, charging efficiency η, data generation rate r_i and the moving speed of the MC v. In order to compare with the upper bound network lifetime whose calculation assumes a fix data packet generation rate over time, we assume $r_{i,t} = r_i$ in the simulation. Note that the calculation of the upper bound of network lifetime does not factor in T_c, u and v; hence, its value remains constant as these parameters change. In addition, we also study the effectiveness of the movement refinement strategy described in Section 3.2.2 through comparing the J-RoC scheme with its naive version that does not have this refinement (tagged as J-RoC-Naive in the figures).

4.2.2.1 Network lifetime with varying T_c

In the proposed scheme, the charging scheduling happens every T_c interval, and the length of T_c affects both the movement overhead of the MC and the amount of energy that an individual node can be charged. To investigate how the scheduling frequency affects the network lifetime, we first evaluate the performance of all the schemes when the T_c interval changes.

Figure 4.3(a) shows that the network lifetime achieved by J-RoC outperforms greedyPlus and J-RoC-Naive under various T_c values and approaches 95% of the upper bound of network lifetime. In Figure 4.3(a), the lifetimes achieved by both the J-RoC and the greedyPlus schemes decrease slightly as T_c increases. This is due to the fact that the charging decisions are made based on the prediction of the network status for the T_c period and they cannot adapt to the network changes effectively if T_c is long. However, even when T_c is as long as 24 hours in our simulation, J-RoC can still achieve 90% of the upper bound of the network lifetime.

Figure 4.3(a) also shows that the difference between the network lifetime achieved by J-RoC and J-RoC-Naive decreases as T_c increases. This is because the number of nodes to be charged in the J-RoC-Naive scheme is independent of the length of T_c. When T_c increases and charging is scheduled less frequently, the MC stays with a node for a longer time and moves

less frequently as well. Therefore, the total movement time decreases and more time could be utilized for charging. Finally, J-RoC and J-RoC-Naive achieve the similar lifetime when T_c is long enough (e.g., 24 hours in the simulation).

4.2.2.2 Network lifetime with varying u

As the value of u affects both the routing metric and the charging schedules in J-RoC, we vary u and measure the achieved network lifetime by all schemes. The results are plotted in Figure 4.3(b).

Compared to $u = 1$, the performance of all schemes improves significantly once u is greater than 1, as the energy-balanced routing avoids depleting the energy of a partial set of nodes and hence elongates the network lifetime. Among them, J-RoC outperforms greedyPlus and J-RoC-Naive under various u values. For instance, when $u = 1024$, greedyPlus, J-RoC-Naive and J-RoC achieve 69%, 82% and 95% of the upper bound of network lifetime, respectively.

When the value of u increases, the performance of J-RoC gradually improves since the charging scheme can guide the routing activities more effectively as described in Equation (3.9). For example, J-RoC achieves 90% of the upper bound of network lifetime when $u = 2$, and achieves 95% of the upper bound when $u \geq 64$.

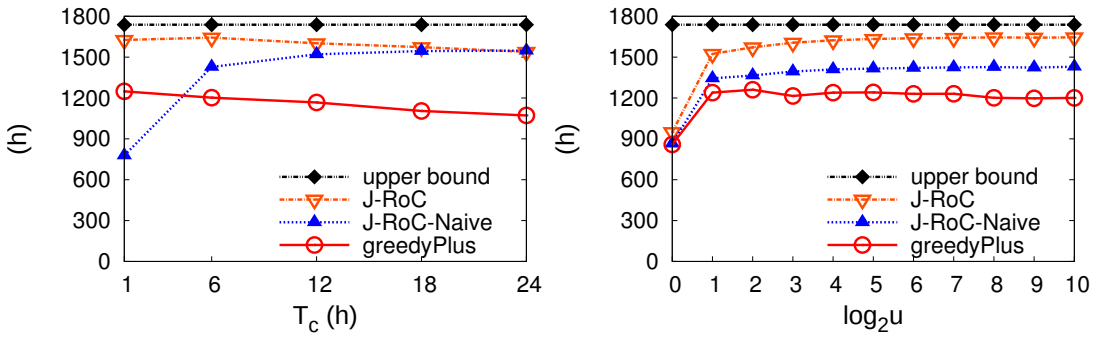

(a) Network lifetime with varying T_c.

(b) Network lifetime with varying u.

Figure 4.3 Achieved network lifetime comparison with varying T_c and u.

4.2.2.3 Network lifetime with varying η

As the energy charging efficiency (e.g., η) depends on how close the MC could reach each sensor node, we show the performance of all the schemes as the charging efficiency η varies in Figure 4.4(a).

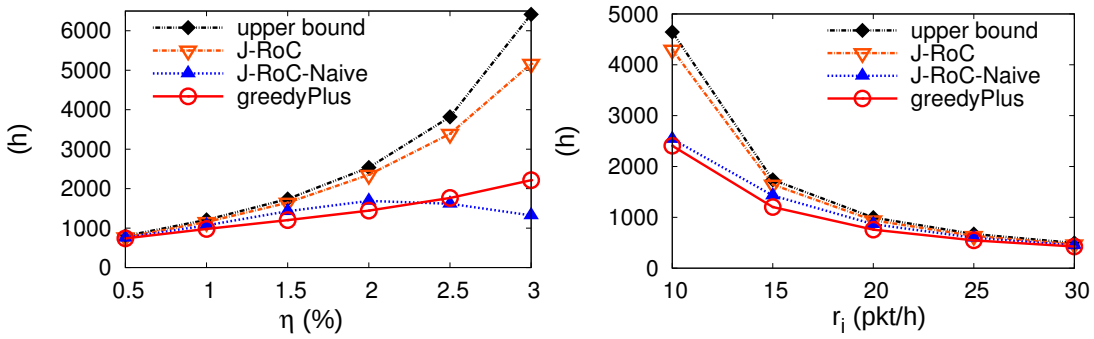

(a) Network lifetime with varying η.

(b) Network lifetime with varying r_i.

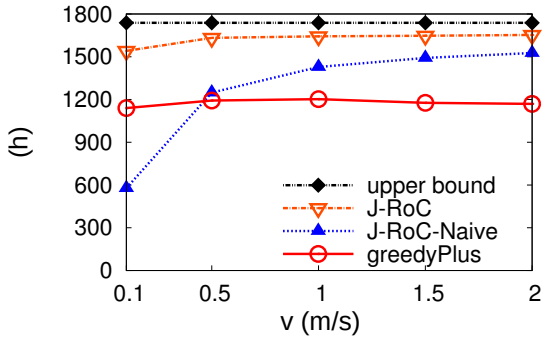

(c) Network lifetime with varying v.

Figure 4.4 Achieved network lifetime comparison with varying η, r_i and v.

Compared to other schemes, the network lifetime achieved by the greedyPlus scheme ascends the most slowly when η increases. This is because a larger η value allows more energy to be captured by a sensor node. Once a node is charged by the MC, its high nodal energy attracts more traffics, which easily makes itself the energy depletion hot-spot and thus the MC has to keep charging and saving it from being depleted. As the trend continues, the charger is stuck with this node and the opportunities of other nodes to be charged are deprived of. The larger

is η, the more intense is this effect. This effect is eliminated in J-RoC which jointly plans the routing and charging activities.

It is also found that the performance of J-RoC-Naive, which does not refine the movement, drops the fastest among all schemes when η is large. This phenomenon can be explained as: the increased η value enables the MC to visit and charge more nodes in one T_c interval, and the movement time increases accordingly without careful movement planning; the J-RoC scheme, on the other hand, alleviates the increasing movement time problem via the movement refinement procedure and outperforms all other schemes.

4.2.2.4 Network lifetime with varying r_i

Different sensory data generation rates may result in different network-wide distribution of energy and workload, which may affect the performance of J-RoC. To study the impact, we vary the values of r_i, measure the network lifetime achieved by all the schemes and plot the results in Figure 4.4(b).

Compared to other schemes, J-RoC performs the best and well adapts to various distribution of energy and workload. It accomplishes around 94% of the upper bound of network lifetime as the value of r_i varies widely. On the other hand, both greedyPlus and J-RoC-Naive achieve a smaller fraction of the upper bound when r_i is small, e.g., only 58% of the upper bound when $r_i = 10$ pkt/h. This is due to the following reasons. When η is fixed, the smaller is r_i, the stronger is the relative charging capability of the MC. J-RoC can make better use of the relatively stronger charging capability to prolong the network lifetime, while the performance of greedyPlus may be degraded because the afore-mentioned effect that the MC is stuck to a energy-depletion hot-spot and J-RoC-Naive may waste time and energy for movement.

4.2.2.5 Network lifetime with varying v

In practice, the moving speed of the MC affects the movement time in all the evaluated schemes and the impact is shown in Figure 4.4(c). Obviously, as the moving speed of the MC increases, less time is wasted on the movement and more energy can be replenished into the network. Therefore, the network lifetime achieved by all schemes improves as v increases.

Since J-RoC conducts the movement refinement, its performance remains almost the same as v changes and achieves about 95% of the upper bound of network lifetime when $v \leq 0.5$ m/s. On the other hand, J-RoC-Naive approaches 88% of the upper bound when $v = 2$ m/s while the achieved fraction is only 33% when $v = 0.1$ m/s. This result illustrates the effectiveness of the movement refinement in Section 3.2.2.

4.2.2.6 Summary

To summarize, the following observations can be obtained from the simulations:

- Compared to greedyPlus, where the MC only passively makes up for the energy deficiency caused by the routing activities to bottleneck nodes, J-RoC improves the network lifetime more significantly due to its proactive guide on the routing activities. The simulation results also show that J-RoC can effectively approach the upper bound network lifetime under various system configurations.

- The movement refinement strategy helps the J-RoC scheme significantly to reduce the movement overhead and achieve a longer network lifetime compared to J-RoC-Naive and greedyPlus.

CHAPTER 5. Discussion

In this thesis, we study a practical and efficient joint routing and charging scheme, called J-RoC, to prolong the sensor network lifetime. We present the design and implementation of the J-RoC scheme and evaluate its effectiveness and advantage on prolonging the sensor network lifetime through both experiments on a prototype system and simulations in large-scale networks, under various configurations. The results show that, through proactively guiding the routing activities and delivering energy to the most energy-demanding places in a joint way, the J-RoC scheme can extend the sensor network lifetime significantly.

Some more issues are left open for future research. For example, the geographical conditions may constrain the movement trajectory of the MC and make some nodes inaccessible. This issue will be factored into the J-RoC scheme. In addition, the J-RoC scheme is designed for a single charger. How to schedule multiple chargers simultaneously is an interesting and more complicated problem, which will also be studied in the future.

BIBLIOGRAPHY

Buettner, M., Yee, G. V., Anderson, E., and Han, R. (2006). X-MAC: a short preamble mac protocol for duty-cycled wireless sensor networks. In *SenSys*.

Chang, J. H. and Tassiulas, L. (2000). Energy conserving routing in wireless ad-hoc networks. In *INFOCOM*.

Chipara, O., Lu, C., Bailey, T. C., and Roman, G.-C. (2010). Reliable clinical monitoring using wireless sensor networks: experiences in a step-down hospital unit. In *SenSys*.

Dantu, K., Rahimi, M., Shah, H., Babel, S., Dhariwal, A., and S., S. G. (2005). Robomote: enabling mobility in sensor networks. In *IPSN*.

Fan, K.-W., Zheng, Z., and Sinha, P. (2008). Steady and fair rate allocation for rechargeable sensors in perpetual sensor networks. In *SenSys*.

Garcia. Online link. http://www.acroname.com.

Gnawali, O., Fonseca, R., Jamieson, K., Moss, D., and Levis, P. (2009). Collection tree protocol. In *SenSys*.

He, S., Chen, J., Fachang, J., Yau, D. K. Y., Xing, G., and Sun, Y. (2011). Energy provisioning in wireless rechargeable sensor networks. In *INFOCOM*.

JOpt.NET. Online link. http://www.dna-evolutions.com.

Jose, S. M., Mur-mir, J. O., Amirtharajah, R., Ch, A. P., and Lang, J. H. (2001). Vibration-to-electric energy conversion. *IEEE Transactions on Very Large Scale Integration (VLSI) Systems*, 9(1):64–76.

Kansal, A., Potter, D., and Srivastava, M. B. (2004). Performance aware tasking for environmentally powered sensor networks. *SIGMETRICS Perform. Eval. Rev.*, 32(1):223–234.

Kar, K., Kodialam, M., Lakshman, T. V., and Tassiulas, L. (2003). Routing for network capacity maximization in energy-constrained ad-hoc networks. In *INFOCOM*.

Kurs, A., Karalis, A., Robert, M., Joannopoulos, J. D., Fisher, P., and Soljacic, M. (2007). Wireless power transfer via strongly coupled magnetic resonances. *Science*, 317:83–86.

Lee, S. H., Lee, S., Song, H., and Lee, H. S. (2009). Wireless sensor network design for tactical military applications: remote large-scale environments. In *MILCOM*.

Lenstra, J. K. and Kan, A. H. G. R. (1981). Complexity of vehicle routing and scheduling problems. In *Networks*.

Li, Q., Aslam, J., and Rus, D. (2001). Online power-aware routing in wireless ad-hoc networks. In *MobiCom*.

Li, Z., Peng, Y., Zhang, W., and Qiao, D. (2010). Study of joint routing and wireless charging strategies in sensor networks. In *WASA*.

Ma, Y., Richards, M., Ghanem, M., Guo, Y., and Hassard, J. (2008). Air pollution monitoring and mining based on sensor grid in london. *Sensors*, 8(6):3601–3623.

Mainwaring, A., Culler, D., Polastre, J., Szewczyk, R., and Anderson, J. (2002). Wireless sensor networks for habitat monitoring. In *WSNA*.

Park, C. and Chou, P. (2006). Ambimax: Autonomous energy harvesting platform for multi-supply wireless sensor nodes. In *SECON*.

Peng, Y., Li, Z., Zhang, W., and Qiao, D. (2010). Prolonging sensor network lifetime through wireless charging. In *RTSS*.

Powercast. Online link. http://www.powercastco.com.

Shi, Y., Xie, L., Hou, Y. T., and Sherali, H. D. (2011). On renewable sensor networks with wireless energy transfer. In *INFOCOM*.

Srinivasan, K., Kazandjieva, M. A., Agarwal, S., and Levis, P. (2008). The beta-factor: Measuring wireless link burstiness. In *SenSys*.

Tong, B., Li, Z., Wang, G., and Zhang, W. (2009a). On-demand node reclamation and replacement for guaranteed area coverage in long-lived sensor networks. In *QShine*.

Tong, B., Li, Z., Wang, G., and Zhang, W. (2010). How wireless power charging technology affects sensor network deployment and routing. In *ICDCS*.

Tong, B., Wang, G., Zhang, W., and Wang, C. (2009b). Node reclamation and replacement for long-lived sensor networks. In *SECON*.

WirelessPowerConsortium. http://www.wirelesspowerconsortium.com/.

Xu, N., Rangwala, S., Chintalapudi, K. K., Ganesan, D., Broad, A., Govindan, R., and Estrin, D. (2004). A wireless sensor network for structural monitoring. In *SenSys*.

Zhang, F., Liu, X., Hackworth, S., Sclabassi, R., and Sun, M. (2009). In vitro and in vivo studies on wireless powering of medical sensors and implantable devices. In *Life Science Systems and Applications Workshop*.

Zhao, J. and Govindan, R. (2003). Understanding packet delivery performance in dense wireless sensor networks. In *SenSys*.